

Differential Phase-Shift Keying Receiver Design Applied to Strong Optical Filtering

Christian Malouin, *Member, IEEE*, Jon Bennike, and Theodore J. Schmidt, *Member, IEEE*

Abstract—We study, via simulation and experiments, the influence of the differential phase-shift keying decoder free spectral range (FSR) when strong optical filtering is considered for the nonreturn-to-zero and return-to-zero modulation formats and show that larger FSR can improve performance.

Index Terms—Differential phase-shift keying (DPSK), optical communication, optical filters, optical modulation, optical receivers, optical signal detection, phase-shift keying.

I. INTRODUCTION

THE DIFFERENTIAL phase-shift keying (DPSK) modulation format has attracted considerable attention in recent years due to its superior optical signal-to-noise (OSNR) sensitivity and fiber nonlinearity tolerance compared to on-off keying formats. It has particularly attracted attention for higher data rate applications: notably 40 Gb/s and beyond. The practical direct detection DPSK receiver architectures considered in this paper require two key components, namely a balanced photodetector and a delay interferometer (DI). These components are quickly reaching a maturity level, enabling the mass production of DPSK-based OC-768/OTU-3 line cards. One critical aspect in any DPSK receiver design is the choice of DI. This choice depends on many factors, including cost, size, control complexity, dense wavelength-division multiplexing (DWDM) system-level considerations (such as channel spacing, single or mixed data rates (e.g., 10 Gb + 40 Gb on the same platform), impact of terminal equipment filters and (reconfigurable) optical add-drop multiplexers [(R)OADMs], and channel plan), and sparing and manufacturing considerations.

The DPSK DI performance has been studied extensively for the return-to-zero (RZ) [1]–[5] and nonreturn-to-zero (NRZ) [6]–[8] formats in the case when optical filtering is weak (no distortion caused by the filtering). Limited papers [9], [10] on DI performance for strong optical filtering can be found in the literature. This subject is of high importance for DWDM systems where the DPSK signals must pass through filters whose effective concatenated optical bandwidths approach, or are below, the data rate. Practical examples include the deployment of OC-768/OTU-3 DPSK signals over OC-192/OTU-2 systems that employs 50-GHz optical filters with (R)OADMs and the deployment over systems that employs a large number

of (R)OADMs, where the concatenated optical bandwidth can quickly go below 50 GHz.

In this paper, we comprehensively study the impact of the free spectral range (FSR) of the DI as a function of additional optical filtering for both the NRZ and RZ DPSK formats at 43 Gb/s. Numerical results are experimentally verified for the NRZ format.

II. BACKGROUND

The DPSK decoding function may be performed using a DI and a balanced detector. The DI works on the principle that the signal is demodulated by comparing the phase of two adjacent bits from a 1-bit DI. The interferometer produces two intensity outputs that are logically conjugated. The DI has a relative time delay difference Y between the two optical fields that is about equal to the symbol duration T . The output called “constructive port” issues a signal $E_c = E_{in}(t) + E_{in}(t - Y)$, and the output called “destructive port” issues a signal $E_d = E_{in}(t) - E_{in}(t - Y)$, where $E_{in}(t)$ is the temporal incident optical field. The effect of the delay Y is to reverse the signals at the two output ports so that the waves cancel (add) at the destructive output port and add (cancel) at the constructive output port when consecutive bits have the same phase (differ by π rad). The fields E_c and E_d can therefore be detected with a direct detection intensity receiver to determine when there is a change in phase in the signal between two consecutive bits and thereby estimate the logical bits carried by the DPSK modulation.

The delay difference Y imposes a transfer function $D(f)$ that has a cosinusoidal/sinusoidal amplitude frequency response from the input to constructive/destructive outputs and is given by

$$D_d^c(f) = \frac{E_d^c(f)}{E_{in}(f)} = \frac{1}{2} \left[1 \pm \varepsilon \exp\left(\frac{j2\pi f}{\text{FSR}}\right) \exp(-j\phi) \right] \quad (1)$$

where ε is related to the DI extinction ratio, ϕ is the optical phase difference between the two arms, FSR is the spectral period of a cycle of the transfer function, which is equal to $1/Y$, and the sign \pm refers to the constructive and destructive ports, respectively. In Fig. 1, $D(f)$ of the constructive and destructive ports are plotted for $\text{FSR}/R = 1.17$ and 1 at $R = 42.84$ Gb/s.

In addition, under a weak optical filtering, DPSK that is used in balanced detection leads to a known benefit of 2 to 3 dB better OSNR sensitivity, compared to single-ended detection [1]. This conclusion is important and will help us to explain some of the following results.

Manuscript received May 23, 2007; revised August 7, 2007.

The authors are with StrataLight Communications, Los Gatos, CA 95032 USA (e-mail: christian@stratalight.com; jon@stratalight.com; ted@stratalight.com).

Digital Object Identifier 10.1109/JLT.2007.907750

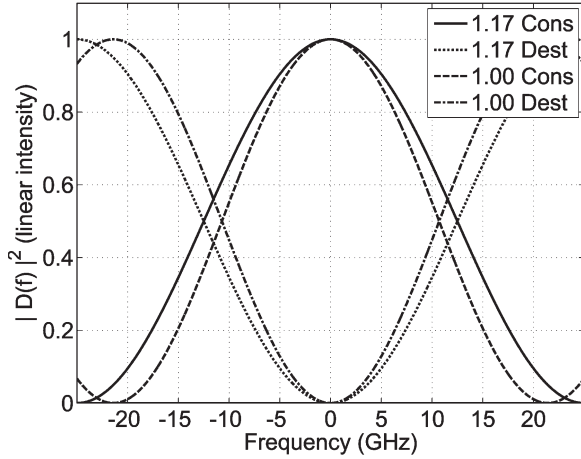


Fig. 1. DI transfer function $|D(f)|^2$ for constructive (Cons) and destructive (Dest) ports for $FSR/R = 1.17$ and 1 at 42.8 Gb/s. Here, $\phi = 0$, and $\varepsilon = 1$.

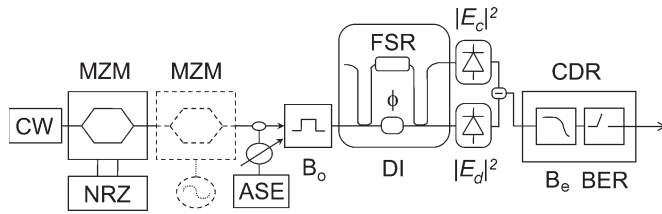


Fig. 2. Experimental and simulation configurations. Solid lines indicate the experimental setup. Dashed lines indicate blocks included in the simulation model for RZ-DPSK.

III. EXPERIMENTAL AND SIMULATION SETUPS

The schematic of the experimental and simulation setups is shown in Fig. 2.

The light from a continuous-wave laser was modulated using a Mach-Zehnder modulator (MZM) in a “push-pull” configuration (biased at null of transmission and with $\pm V\pi$ drive swing for both arms). The MZM was driven by a 43-Gb/s NRZ electrical data sequence from a pseudorandom bit stream (PRBS) of length $2^{31} - 1$. In simulation, RZ signals were generated using a second MZM in a “push-pull” configuration to carve the NRZ signal with a 50% duty cycle. The carver was biased at the middle of transmission and driven with a full clock rate R and $\pm(1/2)V\pi$ drive swing for both arms. The OSNR was set by adding optical amplified spontaneous emission (ASE) noise from a broadband ASE source. The ASE power was adjusted by a variable optical attenuator. At the receiver, the ASE is filtered by an optical filter. Multiple optical filter bandwidths have been tested by using a 75-GHz flat top filter that is concatenated with two thermally detuned 50-GHz interleavers. In simulation, the shape of the resulting filter passband was assumed to be a second-order Gaussian.

Five DI configurations have been experimentally tested. They have a normalized FSR over the bit rate R of 1, 1.17, 1.33, 1.40, and 1.52. In simulation, the FSR/R has been swept from 0.9 to 2. The two outputs of the DI were detected by a balanced photodetector. The photodetector output was coupled to a clock-and-data recovery (CDR) module. The bit error ratio (BER) was reported through a BER analyzer. In simulation, the electrical transfer function of the receiver was considered to be a fourth-

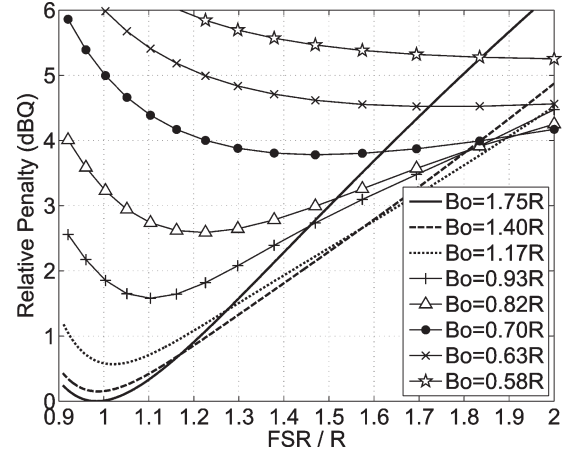


Fig. 3. Simulated relative Q penalty versus FSR/R for different bandwidth B_0 for the 50% RZ-DPSK.

order Bessel-Thompson with 3-dBe bandwidth of $B_e = 0.6R$ (25 GHz), which is consistent with the modeling parameters used in other studies [1], [2], [6].

IV. MODELING AND SIMULATION RESULTS

A Monte Carlo numerical model using error counting was developed. A PRBS length of 2^{10} (repeated ten times before mixing with ASE noise) was used, and errors were accumulated over 200 different noise seeds (equivalent of considering 2 million bits). The optimum time sampling point was found, and the BER versus decision threshold level was swept. To account for phase noise from the CDR, a receiver box time window of $\pm 10\%$ of the bit duration has been assumed. An electrical Q (in decibels) was calculated from the BER value using the following relationship:

$$Q = 20 \log \left[\sqrt{2} \operatorname{erfc}^{-1}(2\text{BER}) \right] \quad (2)$$

where erfc^{-1} is the inverse complementary error function. The model was verified against the results found in the literature [1] and against experimental observations.

The system performance as a function of the FSR of the DI is presented in Sections IV-A (RZ-DPSK) and B (NRZ-DPSK for two Tx electrical bandwidths) for various optical bandwidth B_0 . For these results, the OSNR is set constant to 16 dB (in 0.1-nm resolution bandwidth). For each case, the curves have been normalized to the optimum Q for $B_0 = 1.75R$. For a 50% RZ-DPSK and NRZ-DPSK with Tx bandwidths of 50 and 19 GHz, back-to-back absolute Q performances are 15.4, 15.0, and 14.3 dB, respectively.

A. RZ-DPSK Format

Fig. 3 shows the relative Q penalty versus the normalized FSR/R for different bandwidth B_0 for the 50% RZ-DPSK. As expected, for large B_0 ($\geq 1.75R$), the curve is centered around $FSR/R = 1$ (a perfect 1-bit DI), and a 10% mismatch leads to less than 0.5-dBQ penalty [1]. However, when optical filtering is increased ($B_0 < 1.0R$), two effects are worth mentioning.

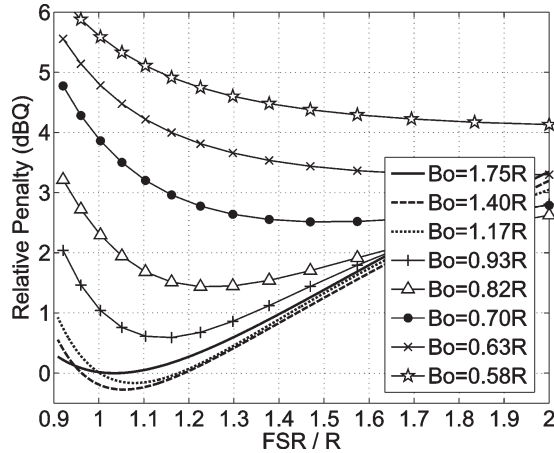


Fig. 4. Simulated relative Q penalty versus FSR/R for different bandwidth B_0 for the NRZ-DPSK with Tx bandwidth of 50 GHz.

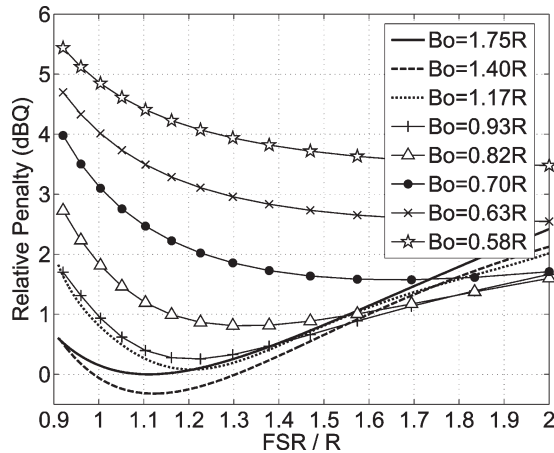


Fig. 5. Simulated relative Q penalty versus FSR/R for different bandwidth B_0 for the NRZ-DPSK with Tx bandwidth of 19 GHz.

First, the penalty due to filtering is always high (> 1 dBQ at $OSNR = 16$ dB). Second, the optimum FSR shifts toward higher values. For strong filtering ($B_0 < 0.7R$), the relative penalty of having a perfect 1-bit DI is higher than 1 dBQ, compared to the optimum FSR DI.

B. NRZ-DPSK Format

For the NRZ-DPSK format, if one wants to accurately predict the DI penalty versus FSR, the rise/fall time (or bandwidth) of the Tx has to be taken into account. For the simulation results shown, a Bessel–Thompson of fourth order with 3-dBe bandwidth of 50 and 19 GHz has been assumed for the Tx electrical bandwidth. Figs. 4 and 5 show the relative Q penalty versus the normalized FSR/R for different B_0 and for Tx bandwidths of 50 and 19 GHz, respectively. When medium to strong optical filtering is considered ($B_0 < 1R$), the same conclusions as in the RZ case can be made: The filtering penalty is always high, and the optimum FSR shifts toward higher values. There is however a slight difference between the two Tx cases for weak optical filtering ($B_0 \geq 1.0R$). For a Tx bandwidth of 50 GHz, the curve is centered around $FSR/R \sim 1$ as in the RZ case. For a Tx bandwidth of 19 GHz, the curve is

not centered around $FSR/R = 1$, as in the previous cases, but around $FSR/R = 1.1$.

We can conclude that the penalty always increases inversely proportional to the optical bandwidth when $B_0 < R$ but can be minimized by increasing the FSR of the DI.

It is also worth mentioning that in Figs. 4 and 5 the slight negative performance penalty obtained for $B_0 = 1.4R$ and $1.17R$ is simply explained by the ASE reduction benefit that is more than the filtering distortion penalty (these bandwidths are closer to a perfect matched filter case compared to $B_0 = 1.75R$ for a given modulation format).

C. Optical Filter Concatenation Rule

In this paper, the optical filter is located at the receiver end only. On real links, filters may be located at the transmitter end (Mux) and at the receiver end (Demux), as well as distributed along the link (OADM and/or ROADM). Apart from the interplay between optical filtering and fiber nonlinear effects (both are functions of the propagation distance), wherein the effect is outside the scope of this paper, we can assume that the modeled filter with a bandwidth B_0 represents an effective filter from a concatenation of all filters present in the link. If the filters have different shapes and/or bandwidths, it is difficult to analytically calculate their effective B_0 . Fortunately, many types of Mux/Demux, interleaver, and (R)OADM are well described by a super-Gaussian function, where the insertion loss spectral shape $IL(f)$ is given by

$$IL(f) = \exp \left(-2^{2n} \ln 2 \left(\frac{f}{B_0^i} \right)^{2n} \right) \tag{3}$$

where B_0^i is the individual filter bandwidth (full-width at half-maximum), and n is the order of the super-Gaussian ($n = 1$ for Gaussian). Assuming that all filters in the link are from the same super-Gaussian order n , the effective bandwidth B_0 from the first up to the N th element is then given by

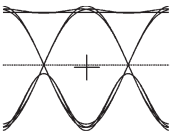
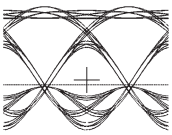
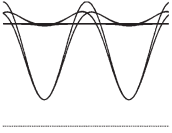
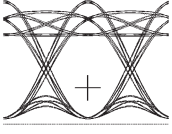
$$B_0 = \left(\frac{1}{N} \right)^{\frac{1}{2n}} B_0^i. \tag{4}$$

Equation (4) is useful in calculating the effective B_0 from the individual filter bandwidth, and consequently, using Figs. 3–5 can predict the optimum FSR/R of the DI.

V. IMPACT OF THE DI FSR

The role of the DI is to differentially decode the DPSK phase and turn it into intensity modulation. For weak optical filtering, a 1-bit DI perfectly decodes the signal. For medium to strong optical filtering, the decoding function of the DI is not needed as much because the optical filter introduces a correlation between adjacent bits, thereby performing the coding/decoding function [11] (precoding occurred at the transmit side). To illustrate this fact, optical eyes are shown in Table I. Four cases are considered, i.e., B_0 is larger ($1.75R$) and smaller ($0.8R$) than R and the signal is detected with and without the use of a DI. In Table I, crosses correspond to the best (time and amplitude)

TABLE I
EYES WITH AND WITHOUT DI AND FOR $B_0 > R$ AND $B_0 < R$

Use of DI	$B_0 > R$	$B_0 < R$
Yes		
No		

sampling point and dashed lines represent the zero amplitude level. For $B_0 > R$ and when a DI is used (top left corner), the balanced optical eye has been decoded and is at its best. For $B_0 > R$ and when no DI is used (bottom left corner), there is no optical eye (the signal is still encoded in phase only). For $B_0 < R$ and when a DI is used (top right corner), the balanced eye has been decoded but is distorted by the optical filtering. For $B_0 < R$ and when no DI is used (bottom right corner), the signal has been decoded, as shown by the presence of the (distorted) single-ended optical eye. Therefore, under tight filtering, the decoding function of the DI is not absolutely required. As we will show, its use is still recommended, primarily because of the better performance of the balanced detection compared to the single-ended detection.

The DI has also a filtering impact (see Fig. 1) on the signal. For weak optical filtering, the DI filtering effect on the performance is minimal. However, in the case where $B_0 < R$, it is important and adds extra signal degradation. To quantitatively illustrate the overall impact of the DI FSR on performance, Q versus B_0 curves are shown in Fig. 6 for balanced detection, constructive and destructive single-ended detections, and for two FSR/ R values of 1.5 (solid lines) and 1.0 (dashed lines). It can be seen that for $B_0 < R$, a DI with an FSR/ R of 1.5 always outperforms that with FSR/ R = 1.0 for all three types of detection (> 1 dBQ for $B_0 < 0.85R$). For $B_0 > R$, we are back to the expected result (for the balanced detection) that a 1-bit DI gives a better performance compared to a DI with FSR/ R = 1.5. Fig. 6 also shows that the destructive port suffers a larger penalty compared to the constructive port. This can be explained by the fact that the DI destructive port can be seen as a high-pass filter (contrary to the constructive port, which corresponds to a low-pass filter). The high-pass filter is then more affected by the strong (“low-pass”) optical filtering. Surprisingly, even if the destructive port is heavily distorted, balanced detection always outperforms constructive single-ended detection. For FSR/ R = 1.5, this difference goes from 2.7 to 1.4 dBQ when B_0/R goes from 1.6 to 0.6.

In summary, under optical filtering where $B_0 < R$, the DI FSR can be increased without impairing its decoding function while lowering the DI inherent filtering effect and maintaining a balanced detection configuration, both of which contribute to improved performance.

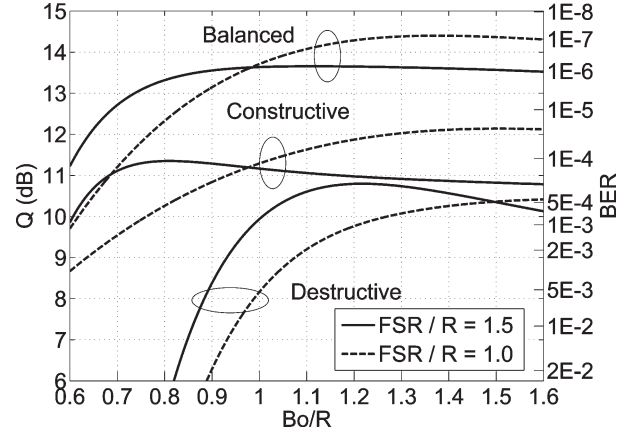


Fig. 6. Q (left axis) and BER (right axis) versus B_0/R for NRZ-DPSK with a DI FSR/ R = 1.5 (solid lines) and 1.0 (dashed lines) for balanced detection and constructive and destructive single-ended detections.

Finally, it is important to note that not only impairments caused by optical filtering can be mitigated by increasing the DI FSR. Any phenomenon producing correlation between consecutive bits, for example impairments due to chromatic dispersion [9] and Tx intersymbol interference (ISI) created by low electrical bandwidth, can be mitigated. That is the reason why under the wide optical filtering case the optimum FSR/ R moved from 1.0 to 1.1 (see Figs. 4 and 5) for a Tx bandwidth of 50 GHz (very low ISI) to 19 GHz (stronger ISI).

For system operators, an important question remaining to be answered is whether the optimum FSR of the DI changes with the link residual chromatic dispersion and accumulated fiber nonlinearity. These questions are addressed in Sections VI and VII, respectively.

VI. IMPACT OF THE DI FSR UNDER RESIDUAL DISPERSION

We use the same setup described in Fig. 2 and add, before the optical filter, a piece of fiber (no nonlinearity) to change the amount of residual chromatic dispersion. Two amounts of residual dispersion have been chosen to produce 1 and 2 dB of OSNR penalty under the wide filtering case. In other words, for these two values of residual dispersion (close to 50 and 70 ps/nm), the OSNR has been increased by 1 and 2 dB, respectively (to bring the performance to the same point), and the Q penalty has been calculated again as a function of the DI FSR for different B_0 values. In Fig. 7, the relative Q penalty for three residual dispersions, which gives 0 dB (solid lines), 1 dB (dashed lines), and 2 dB (dotted lines) of OSNR penalty, is plotted versus FSR/ R for a subset (for clarity) of B_0 values, namely $1.75R$ (without symbols), $0.82R$ (triangles), $0.70R$ (circles), $0.63R$ (crosses), and $0.58R$ (stars). The format is an NRZ-DPSK with a Tx bandwidth of 19 GHz. For $B_0 = 1.75R$, a larger FSR/ R reduces the extra ISI introduced by the dispersion. The FSR/ R increase is only 5% for the 1-dB penalty case and goes up to 27% for the 2-dB case. However, the performance improvement due to the larger FSR/ R is not more than ~ 0.5 dBQ in the wide filtering and 2-dB dispersion penalty cases. For $B_0 \leq 0.82R$, the optimum

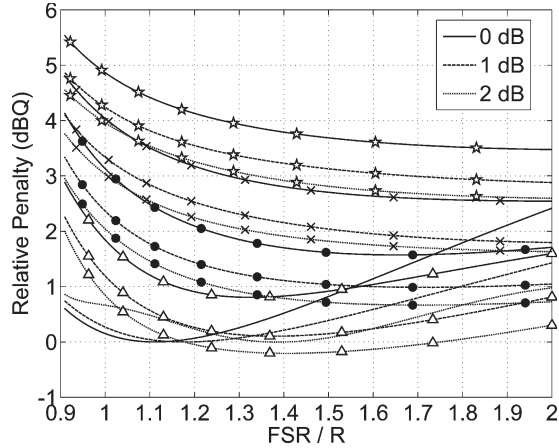


Fig. 7. Simulated relative Q penalty versus FSR/R for 0-dB (solid lines), 1-dB (dashed lines), and 2-dB (dotted lines) residual dispersion penalties and different filter bandwidth B_0 . The filters are $B_0 = 1.75R$ (no symbols), $0.82R$ (triangles), $0.7R$ (circles), $0.63R$ (crosses), and $0.58R$ (stars).

FSR/R is practically unchanged by having up to 2-dB OSNR penalty of residual dispersion. In addition, one can see in Fig. 7 that optical filtering helps in reducing the dispersion penalty, which is indicated by the dashed (1 dB) and dotted (2 dB) lines that are always below the solid (0 dB) line for $B_0 < 1.75R$.

VII. IMPACT OF THE DI FSR UNDER FIBER NONLINEARITY

Another aspect to consider is the accumulated nonlinearity (optical Kerr effect) due to propagation over long or ultralong-haul fiber links. It is, however, cumbersome to study all the possibilities since different nonlinear regimes do exist. Here, we consider only nonlinear effects at 43 Gb/s over terrestrial distances up to 1500 km. We also neglect the nonlinear phase noise effect. In this regime, two single-channel effects are possible, depending (among other things) on the value of the local dispersion of the fiber. They are referred to as intrachannel four-wave mixing (IFWM) for high local dispersion fibers and intrachannel cross-phase modulation for low local dispersion fibers [12]–[14]. Here, we study the most common fiber type, which is the standard single-mode fiber with a local dispersion $D = 16.8$ ps/nm/km and a nonlinear coefficient $\gamma = 1.1$ W⁻¹ · km⁻¹ at 1550 nm, which is capable of producing IFWM. The dispersion maps were chosen to be optimal for 10-Gb/s channels, where the residual dispersion [brought back by dispersion compensating modules (DCM) at every span] should be 27 ps/nm. For the DCM, we used $D = -100$ ps/nm/km and $\gamma = 6.8$ W⁻¹ · km⁻¹ at 1550 nm. The span length is 80 km, the span loss is 21 dB, and the erbium-doped fiber amplifier noise figure was chosen such that the OSNR in 0.1 nm is 17.4 dB at the end of the link for a launch power of 0 dBm. The postcompensation (piece of fiber at the receiver end) has been optimized for each case. The precompensation (piece of fiber at the transmitter end) and the launch powers have been chosen to produce a given performance penalty due to nonlinear propagation. As in Section VI, the same amount of penalty corresponding to 1 and 2 dB of

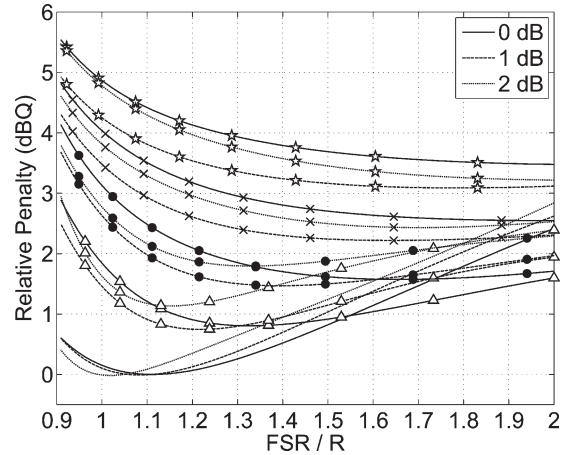


Fig. 8. Simulated relative Q penalty versus FSR/R for 0-dB (solid lines), 1-dB (dashed lines), and 2-dB (dotted lines) nonlinear penalties and different filter bandwidth B_0 . The filters are $B_0 = 1.75R$ (no symbols), $0.82R$ (triangles), $0.7R$ (circles), $0.63R$ (crosses), and $0.58R$ (stars).

OSNR has been considered. Again, the OSNR is adjusted to achieve the same performance as for the wide filtering case.

To avoid the possible interplay between optical filtering and fiber nonlinear effects, the optical filter was placed at the receiver side and its bandwidth B_0 was varied.

Fig. 8 shows the relative Q penalty for three nonlinear strengths, which gives rise to 0 dB (solid lines), 1 dB (dashed lines), and 2 dB (dotted lines) of OSNR penalty versus FSR/R for the same subset (for clarity) of B_0 values, namely $1.75R$ (without symbols), $0.82R$ (triangles), $0.70R$ (circles), $0.63R$ (crosses), and $0.58R$ (stars). The format is still NRZ-DPSK with a Tx bandwidth of 19 GHz. For the 1-dB nonlinear penalty case, the optimum FSR/R is slightly decreased but does not lead to more than 0.1 dBQ of performance degradation compared to the optimum FSR/R found under no nonlinearity. For the 2-dB nonlinear penalty case, the following two regimes can be distinguished: 1) weak-to-moderate filtering ($B_0 \geq 0.7R$) and 2) strong filtering ($B_0 < 0.7R$). For $B_0 \geq 0.7R$, the optimum FSR/R slightly decreases compared to that of the non-nonlinearity case. The reduction is from 10% ($B_0 = 1.75R$) to 20% ($B_0 = 0.82R$ and $0.7R$). For the strong filtering case, the optimum FSR/R is practically unchanged.

The IFWM effect results in amplitude fluctuations, and the propagated waveform appears more “noisy” at the input of the DI. We speculate that this “noise” can be reduced by slightly decreasing the FSR or bandwidth of the DI when the penalty due to the optical filtering is less than the nonlinear penalty.

VIII. EXPERIMENTAL CONFIRMATION

The NRZ-DPSK format at 43 Gb/s has been tested using the setup described in Fig. 2. The residual dispersion and fiber nonlinearity were very low. For these measurements, we used another way of quantifying the performance penalty, i.e., the required OSNR to obtain a BER = 10⁻⁵ was used. The relationship between Q and OSNR penalty is not constant and depends on the signal quality or distortion. For low distortion, there is almost a 1 dBQ per 1 dB OSNR change relation.

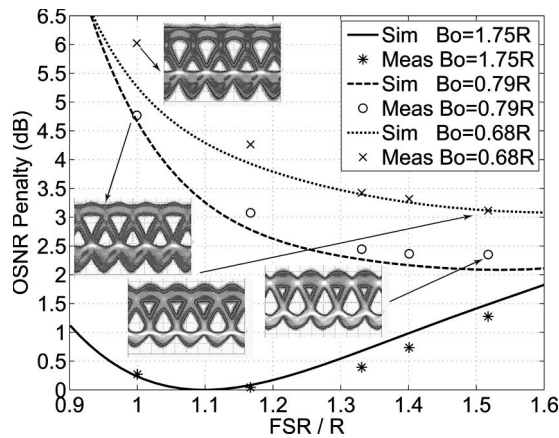


Fig. 9. Measured and simulated OSNR penalties at $\text{BER} = 10^{-5}$ versus DI FSR/R for B_0 of $1.75R$ (solid line and asterisks), $0.79R$ (dashed line and circles), and $0.68R$ (dotted line and crosses).

From low to strong distortion, the “slope” decreases and can be as low as 0.5 dBQ per 1 dB OSNR change. Fig. 9 shows the measured and simulated OSNR penalties (referenced to the best required OSNR, corresponding to the largest optical bandwidth tested) as a function of FSR/R for three optical bandwidths B_0 . These optical bandwidths B_0/R of 1.75, 0.79, and 0.68 are representative of three typical wavelength-division multiplexing (WDM) link architectures. The first WDM link architecture (solid line and asterisks), i.e., $B_0 = 75$ GHz, corresponds to “green-field” links, where no constraint exists on the WDM design and large optical filter passbands can be chosen. The second (dashed line and circles), i.e., $B_0 = 34$ GHz, is a typical 50-GHz Mux + Demux pair. The third (gray line and crosses), i.e., $B_0 = 29$ GHz, is equivalent to using a 50-GHz Mux + Demux pair that is concatenated with multiple 50-GHz (R)OADMs. The electrical eyes (measured using a sampling oscilloscope with a 70-GHz sampling head) from the output of the balanced detector are also shown in Fig. 9.

There is an excellent agreement between measurements (points) and simulations (lines) in terms of the relative OSNR behavior as a function of the FSR and in terms of the absolute performance (predicting the correct penalty when B_0/R decreases from 1.75 to 0.79 and down to 0.68).

For $B_0/R = 1.75$, the measured optimum FSR/R is at 1.1 ± 0.05 , indicating that the Tx bandwidth is close to 19 GHz. In addition, for that case, a DI with an $\text{FSR}/R = 1.17$ ($\text{FSR} = 50$ GHz) performs better than a perfect 1-bit delay decoder. This result is in line with one experimental work [6], where two DIs with $\text{FSR}/R = 1$ and 1.17 have been compared for an NRZ-DPSK format at 42.7 Gb/s, and a similar performance was reported without explaining in detail why this is to be expected.

For $B_0/R = 0.79$, the optical filtering penalty (higher than 2.3 dB of OSNR) is minimized at $\text{FSR}/R \geq 1.4$. Compared to a 1-bit delay, the measured eye is clearly more open for the largest FSR DI tested, translating to a measured 2.5-dB OSNR penalty improvement.

For $B_0/R = 0.68$, the optical filtering penalty is higher than 3.1 dB of OSNR and the optimum FSR/R has shifted toward 1.6. Compared to a 1-bit delay, the measured eye is also clearly

more open for the largest FSR DI tested, translating to a 3-dB OSNR penalty improvement.

IX. CONCLUSION

The optimal DPSK receiver design depends on the optical filtering properties of the DWDM system wherein the channel is to be deployed over. When large effective optical filter bandwidths are present ($B_0 \geq 1.4R$), a perfect 1-bit DI yields optimal results for the RZ-DPSK case. For the NRZ-DPSK format, the optimal DI FSR depends on the particular rise/fall time of the Tx implementation and typically ranges from $\text{FSR}/R = 1$ to 1.1 for a Tx electrical bandwidth ranging from 50 to 19 GHz. When moderate to strong optical filtering is involved ($B_0/R < 1$), an FSR/R greater than 1 and smaller than 1.6 helps reduce the optical filtering penalty for both NRZ-DPSK and RZ-DPSK. We have shown that under tight optical filtering, the DI decoding function is not needed as much. Therefore, the DI FSR can be increased without impairing the decoding function but greatly helps in reducing the inherent DI filtering effect while maintaining the benefit of balanced detection. We have shown via simulation that the optimum FSR/R versus residual dispersion slightly increases ($< 27\%$) under wide filtering but does not change for moderate to strong filtering. Moreover, the optimum FSR/R is practically unchanged when nonlinear penalty up to 2 dB of OSNR and strong filtering ($B_0 < 0.7R$) are considered. For $B_0 > 0.7R$, the optimum FSR/R is not affected by 1-dB nonlinear penalty but decreases by 20% if the nonlinear penalty goes up to 2 dB. Finally, the results have been experimentally verified for the NRZ-DPSK format, and a measured OSNR penalty in excess of 3 dB has been shown for a perfect 1-bit DI compared to the optimum FSR DI.

REFERENCES

- [1] P. J. Winzer and H. Kim, “Degradations in balanced DPSK receivers,” *IEEE Photon. Technol. Lett.*, vol. 15, no. 9, pp. 1282–1284, Sep. 2003.
- [2] P. J. Winzer, S. Chandrasekhar, and H. Kim, “Impact of filtering on RZ-DPSK reception,” *IEEE Photon. Technol. Lett.*, vol. 15, no. 6, pp. 840–842, Jun. 2003.
- [3] A. Agarwal, S. Chandrasekhar, and P. J. Winzer, “Experimental study of photocurrent imbalance in a 42.7-Gb/s DPSK receiver under strong optical filtering,” presented at the Optical Fiber Commun. Conf. (OFC), Anaheim, CA, 2005, Paper OFN4.
- [4] J. H. Sinsky, A. Adamiecki, A. Gnauck, C. A. Burrus, J. Leuthold, O. Wohlgenuth, S. Chandrasekhar, and A. Umbach, “RZ-DPSK transmission using a 42.7-Gb/s integrated balanced optical front end with record sensitivity,” *J. Lightw. Technol.*, vol. 22, no. 1, pp. 180–185, Jan. 2004.
- [5] A. H. Gnauck and P. J. Winzer, “Optical phase-shift-keyed transmission,” *J. Lightw. Technol.*, vol. 23, no. 1, pp. 115–130, Jan. 2005.
- [6] G. Bosco and P. Poggiolini, “The impact of receiver imperfections on the performance of optical direct-detection DPSK,” *J. Lightw. Technol.*, vol. 23, no. 2, pp. 842–848, Feb. 2005.
- [7] J. A. Lazaro, W. Idler, R. Dischler, and A. Klekamp, “BER depending tolerances of DPSK balanced receiver at 43 Gb/s,” in *Proc. IEEE/LEOS Workshop Adv. Modulation Formats*, San Francisco, CA, Jul. 1–2, 2004, pp. 15–16.
- [8] J. Hsieh, C. Ai, V. Chien, X. Liu, A. H. Gnauck, and X. Wei, “Athermal demodulator for 42.7 Gb/s DPSK signals,” in *Proc. ECOC*, 2005, vol. 4, pp. 827–828.
- [9] B. Mikkelsen, C. Rasmussen, P. Mamyshev, and F. Liu, “Partial DPSK with excellent filter tolerance and OSNR sensitivity,” *Electron. Lett.*, vol. 42, no. 23, pp. 1363–1364, Nov. 2006.
- [10] C. Malouin, J. Bennike, and T. Schmidt, “DPSK receiver design—Optical filtering considerations,” presented at the Conf. Optical Fiber Commun. (OFC), Anaheim, CA, 2007, Paper OTHk1.

- [11] D. Penninckx, H. Bissessur, P. Brindel, E. Gohin, and F. Bakhti, "Optical differential phase shift keying (DPSK) direct detection considered as a duobinary signal," in *Proc. ECOC*, 2001, vol. 3, pp. 456–457.
- [12] P. V. Mamyshev and N. A. Mamysheva, "Pulse-overlapped dispersion-managed data transmission and intrachannel four-wave mixing," *Opt. Lett.*, vol. 24, no. 21, pp. 1454–1456, Nov. 1999.
- [13] R.-J. Essiambre, G. Raybon, and B. Mikkelsen, "Pseudo-linear transmission of high-speed signals: 40 and 160 Gb/s," in *Optical Fiber Telecommunication IV-B*. San Diego, CA: Academic, 2002, ch. 6.
- [14] A. Mecozzi, C. B. Clausen, and M. Shtaif, "Analysis of intrachannel nonlinear effects in highly dispersed optical pulse transmission," *IEEE Photon. Technol. Lett.*, vol. 12, no. 4, pp. 392–394, Apr. 2000.



Christian Malouin (M'05) received the Ph.D. degree in physics and optics from the Université Laval, Québec, QC, Canada, in 1996 and the Postdoctoral degree from the Université Paris XI, Orsay, France, where he focused on the characterization of magneto-optical recording media using ultrafast second-order nonlinear effects.

During his Ph.D. dissertation, he developed a novel geometry of four-wave mixing to characterize fast optical nonlinear media. In 1998, he joined Nortel Networks, where he worked on high-capacity transmission systems from 40 to 100 Gb/s. In September 2000, he joined Innovance Networks, where he helped in the design and development of an ultralong-haul all-transparent optical network. Since August 2005, he has been with StrataLight Communications, Los Gatos, CA, where he is currently responsible for the modeling, verification, and prototyping of the optical architecture of existing products and forward-looking products. In particular, his research focuses on transmitter and receiver design/modeling and on the study of advanced modulation formats at high speed using direct detection and coherent schemes.



Jon Bennike received the Master's degree in electrical engineering from the Technical University of Denmark, Lyngby, Denmark, in 2000. His thesis on 40-Gb/s OTDM techniques concluded more than two years of course work and projects within fiber optic communication systems.

From 2000 to 2001, he was a Research Engineer with the Research Center for Communications Optics and Materials (COM), Technical University of Denmark, where he worked on 40-Gb/s clock-recovery methods and jitter characterization of electrooptical oscillators. From 2001 to 2003, he was a Senior Optical Engineer with Mintera Corporation, where he was responsible for new technology evaluation and forward-looking research of advanced modulation formats for 40-Gb/s ultralong-haul transmission systems. Since 2004, he has been a Senior Engineer with the Optical Systems Engineering Group, StrataLight Communications, Los Gatos, CA, where he has been working on the development and deployment of 40-Gb/s subsystems. His interests include high-speed optical communication systems, high-speed digital communication, and signal processing.



Theodore (Ted) J. Schmidt (M'99) received the B.Sc. degree in engineering physics from North Dakota State University, Fargo, in 1992 and the Ph.D. degree in physics from Oklahoma State University, Stillwater, in 1998. His doctoral research centered on the nonlinear optical properties of wide-band-gap semiconductors.

From 1999 to 2000, he was a Staff Engineer with the Network Architecture Division, Williams Communications Group, Tulsa, OK, where he was responsible for the evaluation and selection of Raman-based ultralong-haul transport products for deployment in Williams' nationwide fiber-optic network. From 2000 to 2002, he was a Senior Optical Engineer and Technical Manager with OptiMight Communications (now part of Huawei Technologies), where he was responsible for the development of optical subsystems within OptiMight's ultralong-haul transport product portfolio. Since 2002, he has been the Director of Optical Systems Engineering, StrataLight Communications, Los Gatos, CA, where he is responsible for optical systems research and development. He has authored two book chapters and more than 20 archival journal articles on the nonlinear optical properties of wide-band-gap semiconductors. His research interests include high-speed optical communication systems, optical networking, and semiconductor optical devices.